Flow Visualization and Characterization of Capillary Waves using a Novel Optical Method

Vineet Vishnu Mukim[1], Rune Wiggo Time[1], Andrianifaliana Herimonja Rabenjafimanantsoa[1]
[1]Department of Energy and Petroleum Engineering, University of Stavanger
4036 Stavanger, P.O. box 8600, Norway

ABSTRACT

A novel optical method is presented to reconstruct wave surface topography of parametrically excited finite-amplitude axisymmetric capillary waves. Leveraging refraction of light to magnify amplitude, the method solves the inverse (geometric) optics problem while exploiting the underlying symmetric nature to recreate the entire wave surface uniquely and accurately. Its novelty lies in the simplicity and affordability (laser pointer and smartphone) making it ideal for classroom demonstrations. Subsequently, partial results from ongoing experimental validation are presented.

1. Introduction

Mathematical modeling of waves is integral for gaining insight into real-world phenomena. Despite their omnipresence, water waves were considered unsuitable for elementary courses by Feynman due to their inherent complexities and non-linear behavior. However, capillary waves on liquid-gas interface are described quite accurately by the linear wave theory [1-3]. Resulting equations relate the fundamental liquid properties like surface tension and viscosity to the wave properties like wavelength and attenuation. This fact makes them a great tool for measuring fundamental liquid properties like surface tension and viscosity. Capillary waves are characterized by tiny amplitudes and wavelengths. But different length scales and fine time scales make the measurement difficult.

A classification of wave types along with various methods of generation and detection of waves is given by Slavchov *et al.* [4]. The methods for measurement of waves are broadly classified as "point" methods [5,6] or as "space–time" methods [4,7,8]. The space–time methods provide more data about the wave surface but also require more post-processing. Optical measurement techniques are well suited for space–time methods in view of the relatively large amount of data required. Other advantages of optical techniques are their nonintrusive nature and high resolution. Commonly used optical measurement methods are based on reflection, refraction, diffraction, and interference.

In this short paper, we introduce an optical method [9] for reconstructing the liquid interfaces of parametrically excited finite-amplitude axisymmetric capillary waves. The method stands out for its simplicity, affordability, and yet high accuracy. This is significant as the measurement of sensitive parameters often demands sophisticated and costly instruments. However, our approach is designed to be easily incorporated into classroom or lab settings, relying on minimal and generic assumptions that can be validated experimentally. Classified as partially global (space-time), it employs inverse ray-tracing of a laser sheet refracted through the liquid interface and projected onto a screen. Mathematical formulations and solutions for both forward and inverse problems in geometric optics are presented in subsequent sections.

2. Method

Refraction can be defined as the angular deviation of light rays when passing from one medium to another. This is described mathematically by Snell's law [10]. If the surface is wavy and transient, the surface normal and, hence, the direction of refracted rays also changes over space and time. The angular deviation depends on several factors such as the refractive index of the material, the angle of incidence, the direction of the surface normal, and the depth of the liquid. This well-known phenomenon can be used to study the capillary waves. With sufficient and suitable distance from the surface to a projection screen, even tiny light ray deviations can be detected and measured. The surface disturbances caused by capillary surface waves can then be clearly monitored and measured.

2.1 Forward Problem

The forward problem, i.e., the propagation of light from the source to the bottom and the screen is described in Fig. 1.

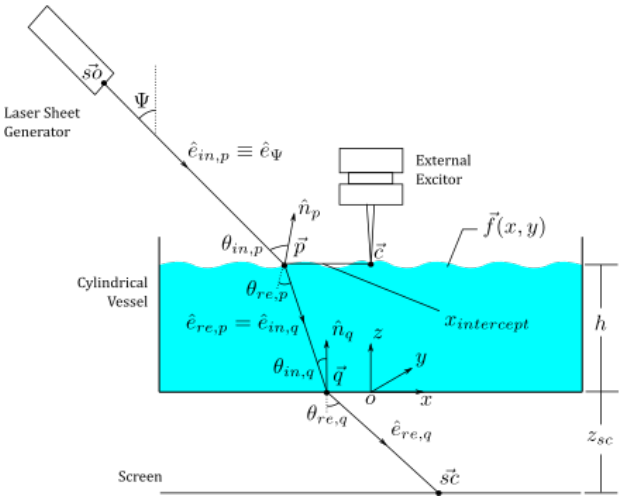

Fig. 1 Forward problem schematic.

It is finding the coordinates of rays hitting the screen when the surface topography, laser source location, laser sheet inclination, refractive index of the liquid, undisturbed (no wave) height of the liquid, and distance between screen and bottom of the vessel are known. Solution (as shown in Fig. 2) can be easily found with

Corresponding author: Vineet Vishnu Mukim
E-mail address: vineet.v.mukim@uis.no

very simple multivariable calculus. This solution is referred to as 'true shape' while assessing the accuracy of inverse problem solution (Fig. 6). Forward problems of this kind are famously known as ray-tracing in the geometric optics and computer graphics community.

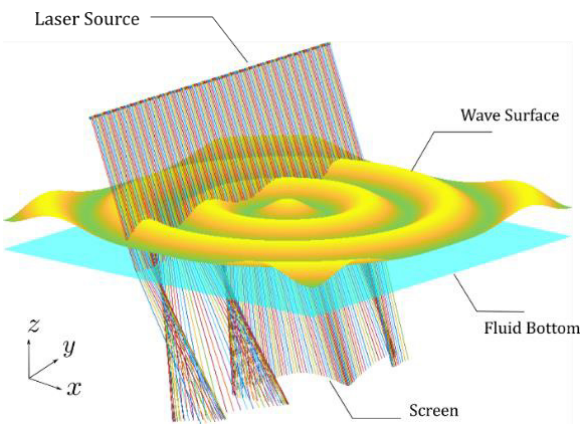

Fig. 2 Forward problem solution.

2.2 Inverse Problem

Compared to the forward problem, an inverse problem can be defined by assuming known screen coordinates and unknown surface topography. Every inverse problem solution requires a proof of existence and uniqueness of the solution. Solution of the forward problem proves the existence of solution using causality. Uniqueness of solution is ensured by leveraging the axisymmetric nature and other simplifications. Mathematically, this means that the surface normal at all points lie in the plane spanned by the corresponding radius vector and the unit vector in the z-direction (coplanarity). Different minimization functions are used to solve the inverse ray-tracing based on Fermat's theorem (Eq. 1), Snell's law (Eq. 2) and implications of axisymmetric nature (Eq. 3). Finally, the problem becomes well-posed ($\mathbb{R}^2 \rightarrow \mathbb{R}^2$) and reduces to finding valid unit surface normal at points on the liquid surface.

Intersection of rays with bottom of liquid is calculated by minimizing the time travelled from $\vec{sc}$ to $\vec{p}_i$,

$$\underset{\vec{q}_i}{\operatorname{argmin}} \left(\frac{|(\vec{q}_i - \vec{sc})|}{\mu_{1,2}} + |(\vec{p}_i - \vec{q}_i)| \right) \tag{1}$$

Surface normal at $\vec{p}_i$ can be calculated by solving,

$$\underset{\alpha_2,\beta_2}{\operatorname{argmin}} |\mu_{1,2} \sin(\theta_{in,i}) - \sin(\theta_{re,i})| \tag{2}$$

Valid unit surface normal direction can be found by invoking its coplanarity with the radius vector,

$$\underset{\vec{p}_i,\hat{n}_i}{\operatorname{argmin}} |((\vec{p}_i - \vec{c}) \times \hat{e}_z) \cdot \hat{n}_i| \tag{3}$$

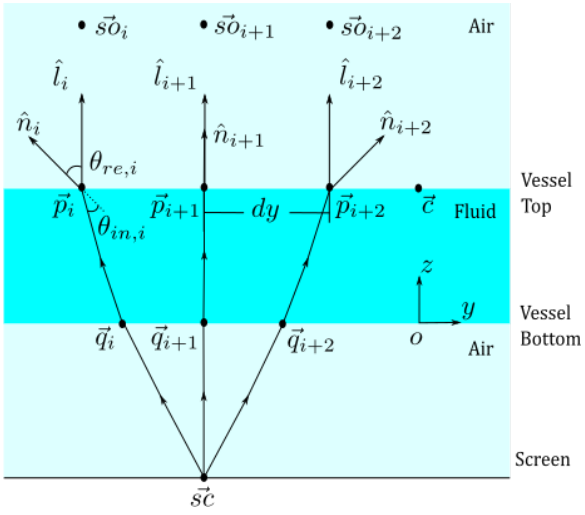

Fig. 3 Inverse problem schematic.

Once valid unit surface normal and its corresponding intercept are determined, the actual surface normal values can be obtained through appropriate scaling. The surface can then be found by numerically integrating the surface normal.

2.3 Experimentation

Fig. 4 illustrates the experimental setup, which differs from the numerical setup in two main aspects, a point diverging laser source and the presence of glass at the bottom of the liquid. The inverse optics algorithm had to be adapted to accommodate these changes.

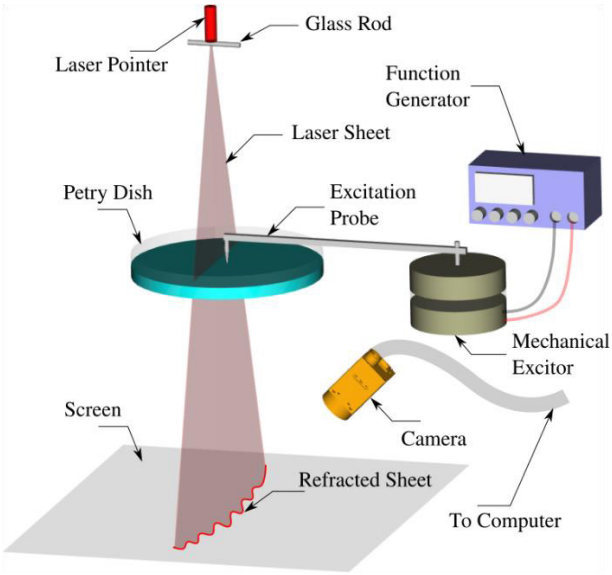

Fig. 4 Experimental setup.

A function generator drives the mechanical vibrator at the desired frequency. A high-speed monochromatic camera captures the refracted sheet on the screen at the bottom. Subsequent post-processing steps are performed using a series of such images, as depicted in Fig. 5.

To calibrate the camera, a collection of images from

various orientations of a checkerboard with a known grid size is needed. The calibration matrix derived from this data is utilized to correct image distortion and convert mean curve image coordinates to physical world coordinates. These physical coordinates are then input into the inverse algorithm to generate the illuminated cross-section. By performing a circular sweep with this data, the complete wave topography (outside circle of radius $x_{intercept}$) can be reconstructed.

As a result of the discrete nature of pixel values in the edge data, the mean finding algorithm approximates the local line normal value. Subsequently, the algorithm determines the curve thickness in the direction of the surface line normal, resulting in the mean curve value in that direction.

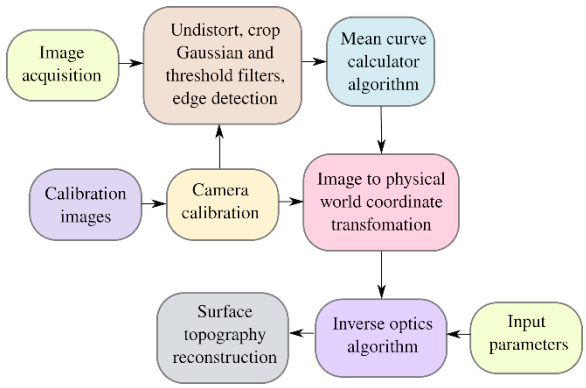

Fig. 5 Block diagram showing various stages of post-processing.

3. Results and Discussion

Conducting a parametric study allowed us to explore the effects of various parameters on the reconstruction error values. Among these parameters, the inclination of the laser sheet and the distance between the center and the illuminated line on the wave surface topography along the x-axis ($x_{intercept}$) have a significant impact on the outcome. The optimal values are found to be zero inclination angle and $x_{intercept} \rightarrow 0$ mm.

Furthermore, a grid sensitivity study reveals the typical trade-off between computation time and error values. Coarse discretization results in errors concentrated at the peaks and valleys of the wave surface cross-section. Thus, the minimum grid discretization appears to be influenced by the minimum curvature value of the wave. Accurate results are obtained by studying both damped and undamped wave surface topographies with varying curvature values (Fig. 6).

Sample images from experimental study at two different times (t and t+δt) are depicted in Fig. 7, illustrating different stages in the post-processing pipeline. It's important to note that the experiments are ongoing, and this work does not include the complete surface reconstruction.

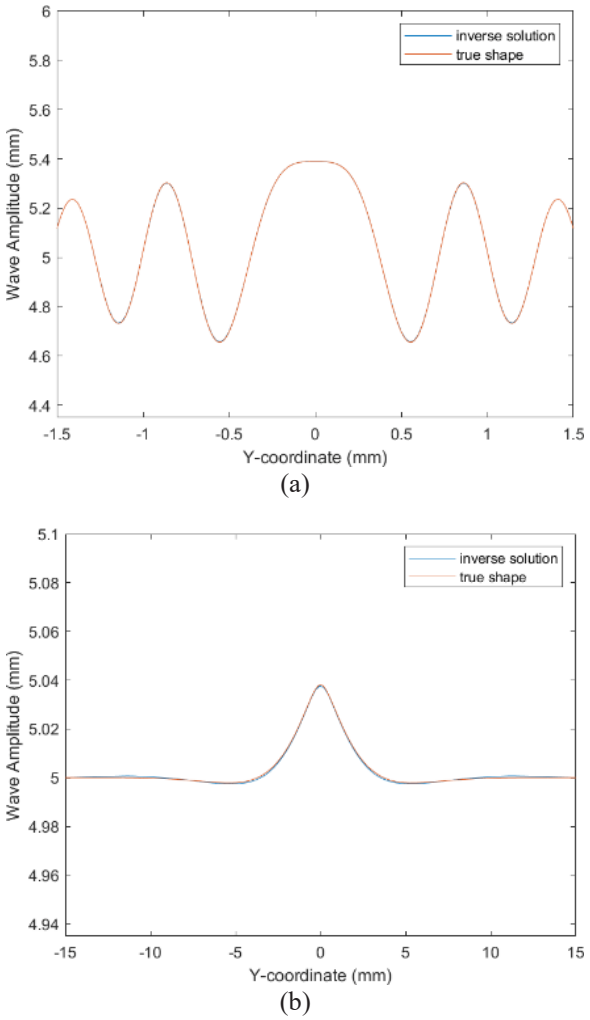

Fig. 6 Comparing solutions of forward and inverse problems for different surface curvatures and damping coefficients (a) λ = 0.5 mm, a = 0.5 mm, dy = 0.025 mm, k = −0.5. (b) λ = 15 mm, a = 0.05 mm, dy = 0.25 mm, k = −0.5.

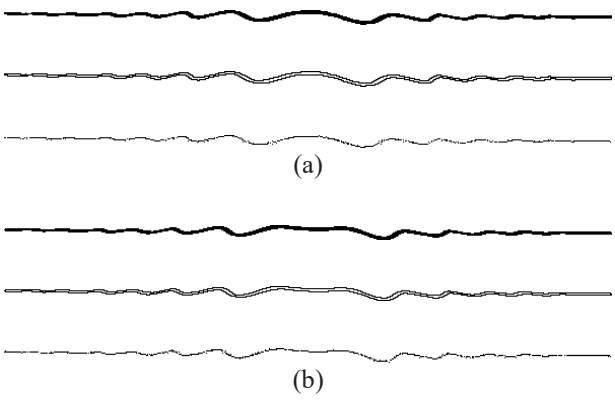

Fig. 7 Results from different stages of post-processing (filtered image, edge detection and mean curve calculator) at times (a) t and (b) t+δt with excitation frequency of 50 Hz.

4. Conclusions

The capillary waves are characterized by very tiny amplitude, which makes it difficult to measure using intrusive methods. A non-intrusive method based on geometric optics is proposed to reconstruct the wave surface with very high accuracy. In this method, a laser sheet illuminates a wave surface and refracts by a varying degree based on the direction of the local surface normal (curvature). The forward problem is defined and solved to trace the rays of light following Snell's law. The data of refracted laser sheet are then used as an input to the inverse problem to obtain valid and correct surface normal values. This method exploits the axisymmetric nature of the wave surface to filter out the best fit surface normal from the available solutions for a given point on the interface to reconstruct the cross-section of the wave surface. Both forward and inverse problems are defined with reasonable assumptions and solved numerically to obtain an excellent agreement in reference analytical (true shape) and reconstructed wave surfaces. This method can work with swapped positions of laser source and screen and prove to be useful in studying axisymmetric surfaces in general.

Subsequently, a comprehensive schematic of the experimental setup and post-processing stages is presented, incorporating practical modifications compared to the forward/inverse problem setup. Essential adjustments have been made to the inverse optics algorithm to accommodate these practical changes. While the experimentation is still in progress, the preliminary results appear promising and align well with the numerical predictions.

Acknowledgement

We acknowledge the support from the Ministry of Education and Research of Norway (Grant No. 8050 IN-12593).

References

[1] H. Lamb, *Hydrodynamics,* University Press, (1924), 625-627.
[2] J. Lighthill, *Waves in Fluids,* Cambridge University Press, (1978), 204-237.
[3] F. Behroozi and N. Podolefsky, *Eur. J. Phys*, 22, (2001), 225-231.
[4] R. I. Slavchov, B. Peychev, and A. S. Ismail, *Phys. Fluids,* 33, (2021), 101303.
[5] F. Behroozi, B. Lambert, and B. Buhrow, *ISA Trans.,* 42, (2003), 3-8.
[6] T. K. Barik, A. Roy, and S. Kar, *Am. J. Phys.,* 73, (2005), 725-729.
[7] X. Zhang, *J. Fluid Mech.,* 289, (1995), 51-82.
[8] F. Moisy, M. Rabaud, and K. Salsac, *Exp. Fluids,* 46, (2009), 1021-1036.
[9] V. V. Mukim, R. W. Time and A. H. Rabenjafimanantsoa, *AIP Advances,* 12 (10), (2022), 105322.
[10] E. Hecht, *Optics,* Addison-Wesley, (2001), 100-111.